Gas seepage pockmark microbiomes suggest the presence of sedimentary coal seams in the Öxarfjörður graben of NE-Iceland

Guðný Vala Þorsteinsdóttir[1,2], Anett Blischke[3], M. Auður Sigurbjörnsdóttir[1], Finnbogi Óskarsson[4], Þórarinn Sveinn Arnarson[5], Kristinn P. Magnússon[1,2,6], and Oddur Vilhelmsson[1,6]

[1]University of Akureyri, Faculty of Natural Resource Sciences, Borgir v. Nordurslod, 600 Akureyri, Iceland.

[2]Icelandic Institute of Natural History, Borgir v. Nordurslod, 600 Akureyri, Iceland

[3]Íslenskar orkurannsóknir / Iceland GeoSurvey (ISOR), Akureyri Branch, Rangarvollum, 600 Akureyri, Iceland

[4]Íslenskar orkurannsóknir / Iceland GeoSurvey (ISOR), Department of Geothermal Engineering, Grensasvegi 9, 108 Reykjavik, Iceland

[5]Orkustofnun / The Icelandic Energy Authority, Grensasvegi 9, 108 Reykjavik, Iceland

[6]Biomedical Center, University of Iceland, Vatnsmyrarvegur 16, 101 Reykjavik, Iceland

Correspondence: Oddur Vilhelmsson, oddurv@unak.is

Abstract

Natural gas seepage pockmarks present ideal environments for bioprospecting for alkane and aromatic degraders, and investigation of microbial populations with potentially unique adaptations to the presence of hydrocarbons. On-shore seepage pockmarks are found at two disparate sites in the Jökulsá-á-Fjöllum delta in NE Iceland. The origin and composition of headspace gas samples from the pockmarks were analysed by GC-MS and stable isotope analysis, revealing a mixture of thermogenic and biogenic gases with considerable inter-site variability. The warmer, geothermally impacted site

displayed a more thermogenic character, comprising mostly methane and CO_2 with minor amounts of higher alkanes. The water chemistry of the pockmark sites was determined, revealing considerable heterogeneity between sites. The geothermally impacted site water contained higher amounts of calcium and zink, and lower amounts of iron than the more biologically impacted site. Microbial communities were analysed by 16S rDNA amplicon sequencing of extracted DNA from the same pockmarks. The bacterial community of the thermogenic gas site was mostly composed of the phyla *Proteobacteria, Chloroflexi* and *Atribacteria,* while the bacterial community of the more biologically impacted site mostly comprised *Proteobacteria, Bacteriodetes* and *Chloroflexi*.

Introduction

Natural gas seepage, the emission of gaseous hydrocarbons from the subsurface, has been studied extensively in the context of petroleum exploration because it can be used as an indicator of petroleum generation in subsurface sediments (1–3). Natural methane gas seepage is the result of subsurface generation or accumulation of methane and the methane concentration in the gas varies according to its source (4). At geothermal and hydrothermal sites, methane is generated by thermogenic processes and seeps up to the surface through cracks and pores, however, the accumulation of methane in deep sea sediments can result in cold seeps or methane hydrates where no direct input of heat is found. This is often linked to biogenic methane which is a product of microbial processes in various anaerobic environments, like bog lakes and sea sediments (5, 6). In many cases the methane generation is of mixed origin, that is both thermogenic and biogenic. For example, methane that is formed during early coalification processes (coal bed methane) is not only of thermogenic origin but also produced by microbes utilizing the lignite (7). In these environments one would expect to find bacteria that participate in methanogenesis and are capable of methane oxidation, respectively.

Where natural methane gas seeps up to the surface, pockmarks can develop, that are a habitat for diverse microorganisms (8) and can be regarded as hotspots for anaerobic oxidation of methane (AOM). AOM is often dependent on archaea and sulphate-reducing bacteria, but can in some cases be driven by bacteria through intra-aerobic-denitrification (9) or possibly reductive dehalogenation (10). Microbial communities of hydrocarbon gas seepage environments have been studied around the world, including the Gulf of Mexico (11), Pacific Ocean Margin (12), Cascadia Margin (13) and Barents Sea (14), mainly because of their sulfate-reducing capabilities and AOM.

In Öxarfjörður bay, NE Iceland, natural gas seepage pockmarks are found both on the seafloor and on shore. Öxarfjörður is located along the lithospheric boundaries of the North-American and the Eurasian plates and forms a graben bounded by the Tjörnes Fracture Zone in the west and the eastern rim of the North Iceland Volcanic Zone in the east. Geothermal activity in Öxarfjörður bay is confined to three major fissure swarms, cross-sectioning the volcanic zone. The area is prevailed by

the river delta of Jökulsá-á-Fjöllum, causing the Öxarfjörður bay to be even more dynamic in nature. Geological settings of the Öxarfjörður area were studied extensively in the 1990s (15–18), leading to the discovery that the methane-rich seepage gas likely originates due to thermal alteration of lignite and coal seams from beneath the 1 km thick sediment (18). Taken together, these studies strongly suggest the presence of sedimentary lignite in the Öxarfjörður graben (19).

Very little geomicrobiological work has thus far been conducted in Iceland, with most environmental microbiology work being bioprospective in nature, often paying little attention to community structures or biogeochemical activity. Notable exceptions include the recent attention to basalt glass bioweathering (20–23), as well as investigations into the microbiota of various geothermally impacted environments such as smectite cones (24, 25), subglacial lakes (26, 27), and various kinds of hot springs and geothermal sinters (28–30). Natural gas seeps such as those found in Öxarfjörður, have thus far not been investigated from a microbiological standpoint despite their unique character which makes them ideal for geomicrobiological studies as both sparsely vegetated geothermal gas seepage pockmarks and colder, more vegetated seepages are found in close proximity to one another. Each methane seep system is thought to be unique in terms of the composition of geological and biological features (8), so taking a snapshot of the microbial community at a methane gas seepage site can provide valuable insight into the dynamics of the system and initiate biological discoveries.

In this article, we report the first microbial analysis of the natural gas seepage pockmarks in Öxarfjörður, providing a platform for future geomicrobiological studies in the area as well as displaying the potential of geomicrobiological studies in Iceland.

Materials and methods

Sampling and in-field measurements

Samples were collected at Skógalón (site SX, 66°09'N, 16°37'W) on August 21st, 2014, and on September 11th, 2015, and at Skógakíll (site AEX, 66°10'N, 16°34'W) on August 13th, 2015 (Fig.1). At site SX, where the natural gas seepage pockmarks are somewhat difficult to distinguish from

ordinary marsh gas pockmarks, sites were selected where pockmarks were visibly active and appeared to form straight lines extending NW-SE. Temperature, pH and conductivity were measured *in-situ* during sampling with hand-held meters. Sediment samples were collected from shallow cores obtained using a corer constructed from a 3-cm diameter galvanized-iron pipe that was hammered into the ground using a sledgehammer, and transferred aseptically to sterile IsoJars (IsoTech laboratories, Champaign, Illinois). Surface soil samples were collected aseptically directly into sterile IsoJars. Water samples were collected aseptically into sterile glass bottles. Gas samples were collected into evacuated double-port glass bottles by means of an inverted nylon funnel connected to silicone rubber tubing. All samples for microbial analysis were immediately put on dry ice where they were kept during transport to laboratory facilities at University of Akureyri where they were either processed immediately or stored in a freezer at -18°C until processing. Samples collected, along with *in-situ* measurements and types of sample are listed in Table 1.

Chemical analysis of geothermal fluids

Dissolved sulphide in the water samples was determined on-site by titration with mercuric acetate using dithizone in acetone as indicator (Arnórsson et al., 2006). Major components in the water samples were determined at the laboratories of Iceland GeoSurvey (ÍSOR) in Reykjavík: Dissolved inorganic carbon was determined by alkalinity titration (pH 8.2 to 3.8), purging with nitrogen gas and back-titration (pH 3.8 to 8.2) as described by Arnórsson et al. (2006). Silica was analysed by colorimetric determination of a silica-molybdate complex at 410 nm using a Jenway 6300 spectrophotometer. Total dissolved solids were determined by gravimetry. Anions were determined by suppressed ion chromatography on a ThermoScientific ICS-2100 with an AS-20 column. Major metals were analysed by atomic absorption spectrometry on a Perkin Elmer 1100B spectrometer. The composition of dry gas was also determined at the ÍSOR laboratories by gas chromatography on a Perkin Elmer Arnel 4019 light gas analyser equipped with HayeSep and MolSieve columns and three TCDs.

The concentration of trace elements in water samples were determined by ICP methods at the ALS Laboratories, Luleå, Sweden. Stable water isotopes (^{2}H and ^{18}O) were determined by mass

spectrometry using a Delta V Advantage IRMS coupled with a Gasbench II at the Institute of Earth Sciences, University of Iceland.

Headspace gas analysis from sediment samples was performed at Applied Petroleum Technologies, Kjeller, Norway, using standard techniques. Briefly as follows:

Sample preparation and extraction. Sediment samples were washed in water to remove mud before extraction using a Soxtec Tecator instrument. Thimbles were pre-extracted in dichloromethane with 7% (vol/vol) methanol, 10 min boiling and 20 min rinsing. The crushed sample was weighed accurately in the pre-extracted thimbles and boiled for 1 hour and rinsed for 2 hours in 80 cc of dichloromethane with 7% (vol/vol) methanol. Copper blades activated in concentrated hydrochloric acid were added to the extraction cups to cause free sulphur to react with the copper. An aliquot of 10% of the extract was transferred to a pre-weighed bottle and evaporated to dryness. The amount of extractable organic matter (EOM) was calculated from the weight of this 10% aliquot.

Deasphaltening. Extracts were evaporated almost to dryness before a small amount of dichloromethane (3 times the amount of EOM) was added. Pentane was added in excess (40 times the volume of EOM/oil and dichloromethane). The solution was stored for at least 12 hours in a dark place before the solution was filtered or centrifuged and the weight of the asphaltenes measured.

GC analysis of gas components. Aliquots of the samples were transferred to exetainers. 0.1-1ml were sampled using a Gerstel MPS2 autosampler and injected into a Agilent 7890 RGA GC equipped with Molsieve and Poraplot Q columns, a flame ionisation detector (FID) and 2 thermal conductivity detector (TCD). Hydrocarbons were measured by FID. H_2, CO_2, N_2, and O_2/Ar by TCD.

Carbon isotope analysis of hydrocarbon compounds and CO_2. The carbon isotopic composition of the hydrocarbon gas components was determined by a GC-C-IRMS system. Aliquots were sampled with a syringe and analysed on a Trace GC2000, equipped with a Poraplot Q column, connected to a Delta plus XP IRMS. The components were burnt to CO_2 and water in a 1000 °C furnace over Cu/Ni/Pt. The water was removed by Nafion membrane separation. Repeated analyses of standards indicate that the reproducibility of $\delta^{13}C$ values is better than 1 ‰ PDB (2 sigma).

Carbon isotope analysis of low concentration methane using the Precon. The carbon isotopic composition of methane was determined by a Precon-IRMS system. Aliquots were sampled with a

148 GCPal autosampler. CO_2, CO and water were removed on chemical traps. Other hydrocarbons than
149 CH_4 and remaining traces of CO_2 were removed by cryotrapping. The methane was burnt to CO_2 and
150 water in a 1000 °C furnace over Cu/Ni/Pt. The water was removed by Nafion membrane separation.
151 The sample preparation system described (Precon) was connected to a Delta plus XP IRMS for $\delta^{13}C$
152 analysis. Repeated analyses of standards indicate that the reproducibility of $\delta^{13}C$ values is better than
153 1 ‰ PDB (2 sigma).
154 **GC of EOM fraction.** A HP7890 A instrument was used. The column was a CP-Sil-5 CB-MS,
155 length 30 m, i.d. 0.25 mm, film thickness 0.25 µm. C20D42 is used as an internal standard.
156 Temperature programme: 50°C (1 min), -4 °C/min, -320 °C (25 min).
157
158 **Metataxonomic community analysis**
159 Total DNA was extracted from sediment samples in duplicates, using the PowerSoil kit (MoBio
160 laboratories) following the manufacturer's protocol. The DNA isolated was measured with Qubit
161 fluorometer (Invitrogen, Carlsbad, CA) to confirm dsDNA in the samples, and a PCR carried out with
162 8F/1522R primers (32) to determine that the bacterial 16S rDNA could be amplified. Paired-end
163 library of the 16S rDNA hypervariable region V3/V4, was sequenced on Illumina MiSeq platform by
164 Macrogen, Netherlands, from 8 samples in total, four from AEX and four from SX. The data was
165 processed and analysed using CLC Genomics Workbench 10.1.1 (https://www.qiagen
166 bioinformatics.com/) and the CLC Microbial Genomics Module 2.5.1, with default parameters.
167 Operational taxonomic units (OTU) were clustered by reference based OTU clustering and tree
168 alignment was performed by using the GreenGenes v.15.5 database for 97% similarity. For statistical
169 analysis only alpha-diversity of samples was performed since the sequencing data only contained
170 technical replicates, which does not allow analyses of beta-diversity. Differential abundance analysis
171 (Likelihood Ratio test) was performed to see statistically significant differences in taxa between
172 sampling sites.
173
174 **Initial culturing and isolation of bacteria**

175 Samples were serially diluted to 10^{-6} in sterile Butterfield's buffer and all dilutions plated in duplicate
176 onto Reasoner's agar 2A (Difco) and several selective and differential media including medium 9K for
177 iron oxidizers (33), Mn medium for manganese oxidizers (990 mL basal agar B [0.42 g NaOAc, 0.1 g
178 peptone, 0.1 g yeast extract, 15 agar, 990 mL sample water, autoclaved and cooled to 50°C], 10 mL
179 pre-warmed filter-sterilized 1 M HEPES at pH 7.5, 100 µL filter-sterilized 100 mM Mn(II)SO_4), Gui
180 medium for laccase producers (990 mL basal agar B, 0,01% guiaicol), Hex medium for hexane
181 degraders (990 mL basal agar B, 1.3 mL filter-sterilized 99 parts hexane/1 part dishwashing
182 detergent), Naph medium for naphthalene degraders (basal agar B with several crystals of naphthalene
183 added to the lid of inverted plates and then sprayed with fast blue for degradation indication), and 2,4-
184 D medium for dichlorophenoxyacetate degraders (basal agar B supplemented with 2 mM 2,4-D).
185 Three atmospheric incubation conditions were used: an unmodified atmosphere in sealed plate bags, a
186 propane-enriched aerobic atmosphere in sealed plate bags flushed daily with propane, and an
187 anaerobic, propane-supplemented atmosphere in anaerobic jars scrubbed of oxygen with a palladium
188 catalyst (BBL GasPak) and monitored for anaerobicity with a resazurin strip. The jars were injected
189 with 100 mL propane through a septum. Plates were incubated in the dark at 5, 15, or 22°C until no
190 new colonies appeared (up to 4 weeks).
191 Colonies were isolated based on isolation medium and colony morphology and streaked onto fresh
192 media and recultured up to three times or until considered pure. Stocks of purified isolates were
193 prepared by suspending a loopful of growth in 1.0 mL 28% (v/v) glycerol and are stored at -70°C in
194 the University of Akureyri culture collection.
195
196 **16S rRNA gene-based identification of cultured strains**
197 For each strain, a minute colony mass or 1 µl of freezer stock was suspended in 25 µl of lysis buffer
198 (1% Triton x-100, 20 mM Tris, 2 mM EDTA, pH 8,0) and incubated for 10 minutes at 95°C in the
199 thermocyler (MJR PTC-200 thermocycler, MJ Research Inc. Massachusetts, USA). The lysis buffer
200 solution (1 µl), or 1 µl of extracted DNA (using UltraClean® Microbial DNA Isolation Kit (MoBio
201 Laboratories, Carlsbad, California, USA)), was used as a DNA template for Polymerase chain
202 reaction (PCR) using Taq DNA-polymerase to amplify the DNA using the ‘universal‘ bacterial

203 primers 8F (5'-AGTTTGATCCTGGCTCAG'3) and 1522R: (5'-AAGGAGGTGATCCAGC CGCA-
204 '3).
205 The PCR reaction was conducted as follows: 95°C for 3 min, followed by 35 cycles of 95°C for 30
206 sec, 50°C for 30 sec and 68°C for 90 sec, then final extension at 68°C for 7 min. The PCR products
207 were loaded on 0,8% agarose gel and run at 100 V for approximately 30 minutes to verify the
208 presence of approximately 1500-bp amplicons.
209 The PCR products were purified for sequencing using 22 µl of sample in 10 µl ExoSap Mix (mix
210 for 50 reactions; 1.25 µl Exonuclease I [20 U/µl], 2.5 µl Antartic phosphatase [5 U/µl] (New England
211 BioLabs Inc.), 496.5 µl distilled H_2O). The products were incubated at 37°C for 30 minutes and
212 heated to 95°C for 5 minutes to inactivate the enzymes in the ExoSap.
213 The purified PCR products were sequenced with BigDye terminator kit on Applied Biosystem
214 3130XL DNA analyser (Applied Biosystems, Foster City, California, USA) at Macrogen Europe,
215 Amsterdam, the Netherlands. Two sequencing reactions were run for each strain, using the primers
216 519F (5'-CAGCAGCCGCGGTAATAC-'3) and 926R (5'-CCGTCAATTCCTTTGAG TTT-'3). The
217 resulting sequences were trimmed using ABI Sequence Scanner (Applied Biosystems), the forward
218 sequence and the reverse complement of the reverse sequence aligned and combined, and taxonomic
219 identities obtained using the EzTaxon server (34).

220 ## Results

221 **Water chemical analysis** revealed several differences in major components at the two sites (Table 2).
222 Although the pH of the water did not differ significantly as judged by a two-tailed Student's t-test,
223 electrical conductivity was nearly 12-fold higher at the AEX site, significant at the 99.5% confidence
224 level. The AEX site water contained more than 420-times as much silica as did the SX site water, and
225 several other ions, such as sodium, potassium chloride and bromide were also found to be present at
226 significantly higher levels at the AEX site, underscoring the more geothermal character of the
227 environment (Table 2).
228

229 **Headspace gas analysis** revealed similar amounts of hydrocarbon gas at the two sites (Table 3).
230 Although methane content was consistently (n=3) found to be lower at the AEX site than at the SX
231 site, the difference was not deemed significant by a two-tailed Student's t-test (not shown). Isotope
232 composition suggests a thermogenic origin of the AEX-site headspace gas, whereas a biogenic origin
233 is suggested for the SX-site headspace gas (Table 3). Thermogenic origin of the AEX gas was further
234 supported by a high methane/ethane ratio (17.8). Both the composition of the headspace gas and the
235 methane isotope composition were similar to those reported by Ólafsson *et al*. for borehole gasses in
236 the Skógalón area (18). EOM fractions showed difference in hydrocarbon content in terms of lower-
237 chain hydrocarbons in AEX and higher amounts of higher-chain hydrocarbons at the SX site (Fig. 2).
238
239 **Metataxanomic analysis.**
240 Four technical replicates from each study site were used to compare the microbial communities in
241 the gas seepage pockmarks of Skógalón (SX) and Skógakíll (AEX). The DNA extraction yielded on
242 average 2,8 µg/ml (± 0,3 µg/ml) and the amplicon library generated on average 42,8 ng/µL (± 1,3
243 ng/µL) of amplicons with the length of 587±5 bp. Over 4 million paired sequences, were analysed and
244 trimmed to the average of 523.241 reads per sample with the length of 301 bp. A total of 595.137
245 reads generated the OTU table after filtering out chimeric sequences, where predicted OTUs were in
246 total 26.786 OTUs (Table 4).
247 Alpha diversity metrics were measured at the depth of 60,000 sequences per sample. The number
248 of OTUs had reached plateau at 25,000 sequences, meaning the dataset was fully sufficient to
249 estimate the diversity of the bacterial communities in the natural seepage pockmarks. The species
250 richness as estimated with Chao1 index and Shannon´s diversity index are shown in Table 4.
251
252 **Taxonomic composition**
253 The focus was set on analysing the most abundant taxa, so after filtering out chloroplast OTUs, the
254 OTUs with the lowest combined abundance (<=1000) were omitted. A total of 14 bacterial phyla was
255 observed as the most abundant at AEX and SX sites, divided up to 23 classes and 45 observed genera

256 (Fig. 3). *Proteobacteria* was the most abundant phylum at both AEX and SX sites, 28% and 30%,
257 respectively. At the AEX site, *Proteobacteria* was followed by *Chloroflexi* (22%) and *Aminicenantes*
258 (10%) at phylum level. At the SX site, the *Bacteroidetes* had significantly higher abundance than in
259 the AEX site, with relative abundance of 24%, followed by *Chloroflexi* (13%).
260 The bacterial community structure differed between sites, but only one class, within the phylum of
261 *Aminicenantes* was found by likelihood ratio analysis to be significantly more abundant at AEX than
262 at the SX site. An order within *Bacteriodetes* was found to be significantly more abundant at the SX
263 site compared to the AEX. The family of *Syntrophaceae* under the class of *Deltaproteobacteria* was
264 more abundant at the SX site with 2,6-fold higher abundance. Three genera within the *Clostridia* class
265 had over 3,0-fold higher abundance at AEX than SX site.
266 **Cultured microbial load.** Plate counts after 7 days at 22°C (Table 5) of samples from site SX
267 indicated the presence of substantial communities of naphthalene and hexane degraders, particularly
268 under aerobic conditions. One hundred and eighty-six colonies were restreaked for isolation in pure
269 culture (Table S1).
270
271 **Isolates.** Putatively facultative chemoautotrophs were surprisingly numerous judging by growth on
272 Mn media, but the extremely restrictive medium 9K only yielded a few colonies, all from sample
273 OX06. Spraying colonies with fast blue confirmed the presence of alpha-naphthol in some of the
274 colonies on Naph-agar, but not all. Strains OX0102 and OX0103 tested positive for naphthalene
275 degradation by fast blue; strains OX0304 and OX0306 tested positive for 2,4-diphenoxyacetate
276 degradation by fast blue. One hundred and six strains have been identified by partial 16S rDNA
277 sequencing using the Sanger method and found to comprise 38 genera in 8 classes (Table 6, Table
278 S2).

279 Discussion

280 The study sites, AEX and SX, were found to be distinct in terms of geochemistry. The AEX site
281 contained higher concentrations of silica, very similar to the concentrations of previous studies on
282 geothermal activity in Öxarfjörður (18) indicating geothermal water coming from the pockmarks. The

283 sodium chloride concentration was higher than in previous studies which implies a mixture of
284 seawater with the geothermal water, however, the pockmarks at AEX are located in a river delta and
285 water samples were taken at the pockmark surface so the intermixture of seawater is not surprising.
286 The water chemistry at SX site shows low concentration of silica indicating no geothermal activity
287 and less intermixture of seawater than at AEX. The stable isotope ratio $\delta^{13}C$ of methane also indicates
288 a biogenic origin of the methane at SX, while at AEX the $\delta^{13}C$ suggests a mixture of thermogenic and
289 biogenic origin of methane, which can most likely be linked to microbial lignite utilization at the site
290 as well as the geothermal activity previously described (18). The hydrocarbon content also shows
291 more complex and higher chain hydrocarbons at SX, that can be related to more vegetation and
292 organic matter accumulation, in contrast with lower-chain hydrocarbons at the AEX site with less
293 vegetation (Figure 2). These geochemical factors underline how disparate the two sites are: the AEX
294 pockmarks containing geothermal groundwater with thermogenic methane generation and the SX
295 pockmarks the result of biogenic natural gas accumulation. The location of SX site and the lining up
296 of the pockmarks can easily suggest thermogenic methane seepage at the site, but the pockmarks
297 explored in this study were identified as marsh gas seepage.
298 The seepage pockmarks were found to harbour diverse microbiotas consisting largely of anaerobic
299 heterotrophs. Given the lack of visible vegetation at the AEX site, available organic matter seems
300 likely to be to a large extent restricted to the gas seep itself. This kind of environment is thus likely to
301 contain a microbial community composed largely of facultative chemolithotrophs and oxidizers of
302 methane, lighter alkanes, and aromatics. These organisms can be valuable for bioremediation of
303 petroleum contamination in basaltic oligotrophic environments such as Icelandic beach
304 environments.The inter-site diversity of both sampling sites was notable, however, several groups of
305 bacteria were shown to vary in relative abundance between the two sampling sites:
306
307 ***Chloroflexi* and methyl halide metabolism**
308 The high relative abundance of *Dehalococcoidia* in the microbial consortia at the study sites,
309 particularly site AEX, is noteworthy and underscores the profound effect that petrochemical seepage
310 has on the composition of the local microbiota. The class *Dehalococcoidia* contains at the present

311 time only one validly described order (*Dehalococcoidales*), one family (*Dehalococcoidaceae*), and
312 three genera (*Dehalococcoides, Dehalobium* and *Dehalogenimonas*), comprising a total of four
313 species, all of which are capable of anaerobic reductive dehalogenation (35–39).
314 A large fraction of the dehalococcoidal OTUs in this study were found to be closely related to the
315 described, dehalorespiring members of this class, with 18% of dehalococcoidal paired-end reads from
316 the AEX site and 48% from the SX site being assigned to the order *Dehalococcoidales* (Table 7), the
317 majority (9120 of 9579) being further assignable to the family *Dehalococcoidaceae*. In further
318 support of dehalorespiration being an important process in the seepage pockmark microbiotas, genera
319 known to contain facultative dehalorespirers, like the betaproteobacterial genus *Dechloromonas* (40)
320 the deltaproteobacterial genus *Anaeromyxobacter* (41), were statistically more abundant at the AEX
321 site. Furthermore, cultured bacteria from the Öxfjörður seeps, while not including *Dehalococcoidia*,
322 do include isolates assigned to genera known to include aerobic facultative dechlorinators, such as
323 *Dechloromonas* and *Shewanella* (Table 7). *Dechloromonas* isolates are capable of anaerobic
324 oxidation of benzene (42) and could possibly be used for bioremediation.
325 The as-yet unnamed and uncharacterized order GIF9, suggested by several environmental studies
326 and highly abundant in the AEX and SX microbiomes (Table 7), may consist of bacteria that posess
327 other metabolic processes than just organohalide respiration. Thus, a recent metagenomic study
328 indicated that some members of this group may be homoacetogenic fermenters that possess a
329 complete Wood-Ljungdahl CO_2 reduction pathway (43). It should thus be stressed that the presence of
330 a large contingent of *Dehalococcoidia*, as was found to be the case in the present study, need not
331 necessarily be indicative of dehlaorespiration constituting a major metabolic activity in the
332 environment under study. Indeed, considerable variation in metabolic characteristics occurs in most
333 well-characterized bacterial classes and hence it must be considered likely that other, perhaps non-
334 dehalorespiring taxa remain to be characterized within this class. Nevertheless, the high abundance of
335 *Dehalococcoidaceae*, as discussed above, does strongly indicate organohalide respiration as an
336 important process in the seepage pockmarks.
337 Recently, it was suggested, in part because of the notable abundance of *Dehalococcoides*, that in
338 certain Antarctic lakebeds, anaerobic methane oxidation may be fuelled by reductive dehalogenation

339 (10). The results of the present study are suggestive of the presence of such an ecosystem in the
340 methane seeps in the Öxarfjörður graben. Methyl halides are often associated with coal combustion
341 (44), further suggesting subsurface interaction of geothermal matter with lignite as a source of
342 chloromethane.

343 Another highly abundant class within the *Chloroflexi* was the *Anaerolineae* (Table 7), a class
344 originally described as consisting of strictly anaerobic chemo-organotrophs (45), and frequently
345 detected in subsurface environments (46–49). However, due to the scarcity of cultured
346 representatives, the metabolic capabilities of this class have remained elusive. A recent study of seven
347 single-cell genomes from deep submarine hydrothermal vent sediments indicated the presence of a
348 Wood-Ljungdahl CO_2 reduction pathway, as well as a number of ABC transporters, and in one case a
349 putative reductive dehalogenase (50). In the present study, the *Anaerolineae* appear fairly diverse,
350 with 81% of *Chloroflexi* paired-end reads being assigned to four orders: the *Anaerolineales* and three
351 putative orders without cultured representation, envOPS12, GCA004, and SHA-20 (Table 7).

352

353 ***Proteobacteria* and the sulfur cycle**

354 The *Proteobacteria* phylum mainly consisted of *Deltaproteobacteria* and *Alphaproteobacteria*
355 (Table 8). The alphaproteobacterial fraction was fairly homogeneous, consisting mostly of reads
356 assigned to the order Rhizobacteriales, of which 77% could be assigned to a single genus, *Bosea,* a
357 genus of chemolithoheterotrophs noted for their ability to oxidize inorganic sulfur compounds (51).
358 The deltaproteobacterial fraction was found to be more diverse although most of the OTUs could be
359 assigned to either of two orders, the *Syntrophobacterales* and the *Desulfobacterales* (Table 8), both of
360 which contain mostly, albeit not exclusively, sulfate-reducing organisms.

361 The *Syntrophobacterales,* known to be frequently associated with anoxic aquatic environments
362 (52), are significantly enriched in the SX marshland site as compared to the AEX site, perhaps
363 reflecting an influx of marshland-associated bacteria into the seepage pockmark environment. Most of
364 the Syntrophomonadales reads (77%) can be assigned to the family *Syntrophaceae*, which contains
365 both sulfate-reducing and non-sulfate-reducing bacteria (53). Many of the *Syntrophaceae* reads (59%)
366 could not be confidently assigned to genera, rendering the question of the importance of sulfate

367 reduction of this taxon in the seepage pockmarks unresolved. However, taken together with the high
368 abundance of the sulfate-reducing order *Desulfobacterales*, sulfate reduction is likely to be a major
369 process in the seepage pockmarks, likely supporting AOM consortia. Families within
370 *Desulfobacterales* have been reported to actively oxidizing short and long chain alkanes and are
371 suggested to be the key alkane degraders in marine seeps (54). Furthermore, considering the high
372 abundance of the sulfur-oxidizing *Bosea*, we can surmise that *Proteobacteria* consitute an important
373 driver of sulfur cycling within the seepage pockmark microbiota.
374
375 **Is anaerobic oxidation of methane carried out by *Atribacteria* in the seepage pockmarks?**
376 *Atribacteria* (group 'OP9') are often found to be predominant in methane-rich anaerobic
377 environments such as marine sediments and subseafloor "mud volcanoes" (55, 56). Although they
378 have not been directly linked to AOM in these environments, they have been suggested to mediate
379 AOM in some cold seep environments (10). In general, the *Atribacteria* are thought to play
380 heterotrophic roles, likely fermentative (55, 57), but a single-cell genomics studies on representative
381 *Atribacteria* suggests that these organisms may be indirectly responsible for methane production
382 through the production of acetate or CO_2 (55, 58).
383
384 **Concluding remarks**
385 This study reveals natural gas seeps of biogenic origin in Öxarfjörður in addition to known
386 geothermal gas seepage pockmarks in the Jökulsá-á-Fjöllum river delta. The microbial communities
387 associated with the pockmarks show higher biodiversity at biogenic gas seepage than in thermogenic
388 gas seepage pockmarks. The abundant taxa in the pockmarks indicate that the microbial community is
389 most likely involved in hydrocarbon degradation linked to sulfur cycling and AOM, and the
390 abundance of *Dehalococcoidia* suggests the presence of anaerobic reductive dehalogenation in natural
391 gas seepage pockmarks of thermogenic origin. Further studies are needed to demonstrate the
392 connection between the gas origin and the pockmark microbiota, establishing the need for further
393 geomicrobiological research in Icelandic natural gas seeps.
394

Acknowledgments

This work was funded by Orkustofnun and Orkurannsoknarsjodur Landsvirkjunar. Thanks to Geir Hansen & Co. at Applied Petroleum Technology.

References

1. Link WK. 1952. Significance of oil and gas seeps in world oil exploration. Am Assoc Pet Geol Bull 36:1505–1540.
2. Jones, V. T., & Drozd RJ. 1983. Predictions of oil or gas potential by near-surface geochemistry. Am Assoc Pet Geol Bull 67:932–952.
3. Abrams MA, Dahdah NF. 2010. Surface sediment gases as indicators of subsurface hydrocarbons - examining the record in laboratory and field studies. Mar Pet Geol 27:273–284.
4. Etiope G, Feyzullayev A, Baciu CL. 2009. Terrestrial methane seeps and mud volcanoes: A global perspective of gas origin. Mar Pet Geol 26:333–344.
5. Zengler K, Richnow HH, Rosselló-Mora R, Michaelis W, Widdel F. 1999. Methane formation from long-chain alkanes by anaerobic microorganisms. Nature 401:266–269.
6. Martini AM, Budai JM, Walter LM, Schoell M. 1996. Microbial generation of economic accumulations of methane within a shallow organic-rich shale. Nature 383:155–158.
7. Ritter D, Vinson D, Barnhart E, Akob DM, Fields MW, Cunningham AB, Orem W, McIntosh JC. 2015. Enhanced microbial coalbed methane generation: A review of research, commercial activity, and remaining challenges. Int J Coal Geol 146:28–41.
8. Zhang CL, Lanoil B. 2004. Geomicrobiology and biogeochemistry of gas hydrates and cold seeps. Chem Geol 205:187–194.
9. Ettwig KF, Butler MK, Le Paslier D, Pelletier E, Mangenot S, Kuypers MMM, Schreiber F, Dutilh BE, Zedelius J, de Beer D, Gloerich J, Wessels HJCT, van Alen T, Luesken F, Wu ML, van de Pas-Schoonen KT, Op den Camp HJM, Janssen-Megens EM, Francoijs K-J, Stunnenberg H, Weissenbach J, Jetten MSM, Strous M. 2010. Nitrite-driven anaerobic methane oxidation by oxygenic bacteria. Nature 464:543–548.

10. Saxton MA, Samarkin VA, Schutte CA, Bowles MW, Madigan MT, Cadieux SB, Pratt LM, Joye SB. 2016. Biogeochemical and 16S rRNA gene sequence evidence supports a novel mode of anaerobic methanotrophy in permanently ice-covered Lake Fryxell, Antarctica. Limnol Oceanogr 61:S119–S130.

11. Mills HJ, Martinez RJ, Story S, Sobecky PA, Sobecky A. 2005. Characterization of Microbial Community Structure in Gulf of Mexico Gas Hydrates : Comparative Analysis of DNA- and RNA-Derived Clone Libraries Characterization of Microbial Community Structure in Gulf of Mexico Gas Hydrates : Comparative Analysis of DNA-. Appl Environ Microbiol 71:3235–3247.

12. Inagaki F, Nunoura T, Nakagawa S, Teske A, Lever M, Lauer A, Suzuki M, Takai K, Delwiche M, Colwell FS, Nealson KH, Horikoshi K, D'Hondt S, Jørgensen BB. 2006. Biogeographical distribution and diversity of microbes in methane hydrate-bearing deep marine sediments on the Pacific Ocean Margin. Proc Natl Acad Sci U S A 103:2815–20.

13. Knittel K, Boetius A, Lemke A, Eilers H, Lochte K, Pfannkuche O, Linke P, Amann R. 2003. Activity, Distribution, and Diversity of Sulfate Reducers and Other Bacteria in Sediments above Gas Hydrate (Cascadia Margin, Oregon). Geomicrobiol J 20:269–294.

14. Niemann H, Lösekann T, de Beer D, Elvert M, Nadalig T, Knittel K, Amann R, Sauter EJ, Schlüter M, Klages M, Foucher JP, Boetius A. 2006. Novel microbial communities of the Haakon Mosby mud volcano and their role as a methane sink. Nature 443:854–858.

15. Flóvenz ÓG, Gunnarsson K. 1991. Seismic crustal structure in Iceland and surrounding area. Tectonophysics 189:1–17.

16. Gunnarsson K. 1998. Sedimentary basins of the N-Iceland shelf. Draft Version for Discussion (April–May 1998). Report OS-98014. Reykjavík.

17. Friðleifsson GÓ. 1994. Geothermal gradient and hydrothermal systems off North Iceland. Statement GÓF-94-05. Reykjavík.

18. Ólafsson M, Friðleifsson GÓ, Eiríksson J, Sigvaldason H, Ármansson H. 1993. On the origin of organic gas in Öxarfjörður, NE-Iceland. Report No. OS-93015/JHD-05. Reykjavík.

19. Richter B, Gunnarsson K. 2010. Overview of hydrocarbon related research in Tjörnes.

450 GagnavefsjaIs.
451 20. Kelly LC, Cockell CS, Herrera-Belaroussi A, Piceno Y, Andersen G, DeSantis T, Brodie E,
452 Thorsteinsson T, Marteinsson VV, Poly F, LeRoux X. 2011. Bacterial Diversity of Terrestrial
453 Crystalline Volcanic Rocks, Iceland. Microb Ecol 62:69–79.
454 21. Cockell CS, Olsson K, Knowles F, Kelly L, Herrera A, Thorsteinsson T, Marteinsson V. 2009.
455 Bacteria in Weathered Basaltic Glass, Iceland. Geomicrobiol J 26:491–507.
456 22. Cockell CS, Kelly LC, Marteinsson V. 2013. Actinobacteria—an ancient phylum active in
457 volcanic rock weathering. Geomicrobiol J 30:706–720.
458 23. Kelly LC, Cockell CS, Thorsteinsson T, Marteinsson V, Stevenson J. 2014. Pioneer Microbial
459 Communities of the Fimmvörðuháls Lava Flow, Eyjafjallajökull, Iceland. Microb Ecol
460 68:504–518.
461 24. Marteinsson V, Kristjánsson JK, Kristmannsdóttir H, Dahlquist M, Sæmundsson K,
462 Hannington M, Pétursdóttir SK, Geptner A, Stoffers P. 2001. Discovery and description of
463 giant submarine smectite cones on the seafloor in Eyjafjordur, Northern Iceland, and a novel
464 thermal microbial habitat. Appl Environ Microbiol 67:827–833.
465 25. Geptner A, Kristmannsdóttir H, Kristjánsson J, Marteinsson V. 2002. Biogenic saponite from
466 an active submarine hot spring, Iceland. Clays Clay Miner 50:174–185.
467 26. Gaidos E, Marteinsson V, Thorsteinsson T, Johannesson T, Runarsson AR, Stefansson A,
468 Glazer B, Lanoil B, Skidmore M, Han S, Miller M, Rusch A, Foo W. 2009. An oligarchic
469 microbial assemblage in the anoxic bottom waters of a volcanic subglacial lake. Isme J 3:486–
470 497.
471 27. Gaidos E, Lanoil B, Thorsteinsson T, Graham A, Skidmore M, Han SK, Rust T, Popp B. 2004.
472 A viable microbial community in a subglacial volcanic crater lake, Iceland. Astrobiology
473 4:327–344.
474 28. Hobel CF V, Marteinsson V, Hreggviðsson GÓ, Kristjánsson JK. 2005. Investigation of the
475 microbial ecology of intertidal hot springs by using diversity analysis of 16S rRNA and
476 chitinase genes. Appl Environ Microbiol 71:2771–2776.
477 29. Tobler DJ, Benning LG. 2011. Bacterial diversity in five Icelandic geothermal waters:

478 temperature and sinter growth rate effects. Extremophiles 15:473.
479 30. Pétursdóttir SK, Björnsdóttir SH, Hreggviðsson GÓ, Hjörleifsdóttir S, Kristjánsson JK. 2009.
480 Analysis of the unique geothermal microbial ecosystem of the Blue Lagoon. FEMS Microbiol
481 Ecol 70:425–432.
482 31. Sæmundsson K, Hjartarson Á, Kaldal I, Sigurgeirsson MA, Kristinsson SG, S V. 2017.
483 Jarðfræðikort af Norðurgosbelti. Nyrðri hluti. 1:100.000. Íslenskar Orkurannsóknir and
484 Landsvirkjun., Reykjavík.
485 32. Lane DJ. 1991. 16S/23S rRNA sequencing. En: Stackebrandt E., Goodfellow M. (ed), Nucleic
486 acid techniques in bacterial systematics. John Wiley Sons, New York, NY 115–175.
487 33. Silverman MP, Lundgren DG. 1959. Studies on the chemoautotrophic iron bacterium
488 Ferrobacillus ferrooxidans. J Bacteriol 77:642–647.
489 34. Kim O-S, Cho Y-J, Lee K, Yoon S-H, Kim M, Na H, Park S-C, Jeon YS, Lee J-H, Yi H, Won
490 S, Chun J. 2012. Introducing EzTaxon-e: a prokaryotic 16S rRNA gene sequence database
491 with phylotypes that represent uncultured species. Int J Syst Evol Microbiol 62:716–21.
492 35. Löffler F, Yan J, Ritalahti K, Adrian L, Edwards E, Konstantinidis K, Müller J, Fullerton H,
493 Zinder S SA. 2013. Dehalococcoides mccartyi gen. nov., sp. nov., obligately organohalide-
494 respiring anaerobic bacteria relevant to halogen cycling and bioremediation, belong to a novel
495 bacterial class, Dehalococcoidia classis nov., order Dehalococcoidales ord. nov. and famil. Int
496 J Syst Evol Microbiol 63:625–635.
497 36. Bowman KS, Nobre MF, da Costa MS, Rainey F a, Moe WM. 2012. Dehalogenimonas
498 alkenigignens sp. nov., a chlorinated alkane dehalogenating bacterium isolated from
499 groundwater. Int J Syst Evol Microbiol.
500 37. Moe WM, Yan J, Nobre MF, da Costa MS, Rainey FA. 2009. Dehalogenimonas
501 lykanthroporepellens gen. nov., sp. nov., a reductively dehalogenating bacterium isolated from
502 chlorinated solvent-contaminated groundwater. Int J Syst Evol Microbiol 59:2692–2697.
503 38. May HD, Sowers KR. 2016. "Dehalobium chlorocoercia" DF-1-from discovery to application,
504 p. 563–586. *In* Organohalide-Respiring Bacteria.
505 39. Nuzzo A, Negroni A, Zanaroli G, Fava F. 2017. Identification of two organohalide-respiring

506 Dehalococcoidia associated to different dechlorination activities in PCB-impacted marine
507 sediments. Microb Cell Fact 16:127.
508 40. Achenbach LA, Michaelidou U, Bruce RA, Fryman J, Coates JD. 2001. Dechloromonas
509 agitata gen. nov., sp. nov. and Dechlorosoma suillum gen. nov., sp. nov., two novel
510 environmentally dominant (per)chlorate-reducing bacteria and their phylogenetic position. Int
511 J Syst Evol Microbiol 51:527–533.
512 41. Sanford RA, Cole JR, Tiedje JM. 2002. Characterization and description of Anaeromyxobacter
513 dehalogenans gen. nov., sp. nov., an aryl-halorespiring facultative anaerobic myxobacterium.
514 Appl Environ Microbiol 68:893–900.
515 42. Coates JD, Chakraborty R, Lack JG, O'Connor SM, Cole KA, Bender KS, Achenbach LA.
516 2001. Anaerobic benzene oxidation coupled to nitrate reduction in pure culture by two strains
517 of Dechloromonas. Nature 411:1039–1043.
518 43. Hug LA, Castelle CJ, Wrighton KC, Thomas BC, Sharon I, Frischkorn KR, Williams KH,
519 Tringe SG, Banfield JF. 2013. Community genomic analyses constrain the distribution of
520 metabolic traits across the Chloroflexi phylum and indicate roles in sediment carbon cycling.
521 Microbiome 1:22.
522 44. McCulloch A, Aucott ML, Benkovitz CM, Graedel TE, Kleiman G, Midgley PM, Li Y-F.
523 1999. Global emissions of hydrogen chloride and chloromethane from coal combustion,
524 incineration and industrial activities: Reactive Chlorine Emissions Inventory. J Geophys Res
525 104:8391–8403.
526 45. Yamada T, Sekiguchi Y, Hanada S, Imachi H, Ohashi A, Harada H, Kamagata Y. 2006.
527 Anaerolinea thermolimosa sp. nov., Levilinea saccharolytica gen. nov., sp. nov. and Leptolinea
528 tardivitalis gen. nov., sp. nov., novel filamentous anaerobes, and description of the new classes
529 Anaerolineae classis nov. and Caldilineae classis nov. in the . Int J Syst Evol Microbiol
530 56:1331–1340.
531 46. Schippers A, Kock D, Höft C, Köweker G, Siegert M. 2012. Quantification of Microbial
532 Communities in Subsurface Marine Sediments of the Black Sea and off Namibia. Front
533 Microbiol 3:16.

534 47. Galand PE, Potvin M, Casamayor EO, Lovejoy C. 2010. Hydrography shapes bacterial
535 biogeography of the deep Arctic Ocean. ISME J 4:564–576.
536 48. Kato S, Kobayashi C, Kakegawa T, Yamagishi A. 2009. Microbial communities in iron-silica-
537 rich microbial mats at deep-sea hydrothermal fields of the Southern Mariana Trough. Environ
538 Microbiol 11:2094–2111.
539 49. Cleary DFR, Coelho FJRC, Oliveira V, Gomes NCM, Polónia ARM. 2017. Sediment depth
540 and habitat as predictors of the diversity and composition of sediment bacterial communities in
541 an inter-tidal estuarine environment. Mar Ecol 38:e12411.
542 50. Fullerton H, Moyer CL. 2016. Comparative Single-Cell Genomics of Chloroflexi from the
543 Okinawa Trough Deep-Subsurface Biosphere. Appl Environ Microbiol 82:3000–3008.
544 51. Das SK. 2015. BoseaBergey's Manual of Systematics of Archaea and Bacteria. John Wiley &
545 Sons, Ltd.
546 52. Kuever J, Rainey FA, Widdel F. 2015. Syntrophobacterales ord. novBergey's Manual of
547 Systematics of Archaea and Bacteria. John Wiley & Sons, Ltd.
548 53. Kuever J, Rainey FA, Widdel F. 2015. Syntrophaceae fam. nov.Bergey's Manual of
549 Systematics of Archaea and Bacteria. John Wiley & Sons, Ltd.
550 54. Kleindienst S, Herbst F-A, Stagars M, von Netzer F, von Bergen M, Seifert J, Peplies J,
551 Amann R, Musat F, Lueders T, Knittel K. 2014. Diverse sulfate-reducing bacteria of the
552 Desulfosarcina/Desulfococcus clade are the key alkane degraders at marine seeps. ISME J
553 8:2029–2044.
554 55. Carr SA, Orcutt BN, Mandernack KW, Spear JR. 2015. Abundant Atribacteria in deep marine
555 sediment from the Adélie Basin, Antarctica. Front Microbiol 6:872.
556 56. Hoshino T, Toki T, Ijiri A, Morono Y, Machiyama H, Ashi J, Okamura K, Inagaki F. 2017.
557 Atribacteria from the Subseafloor Sedimentary Biosphere Disperse to the Hydrosphere
558 through Submarine Mud Volcanoes. Front Microbiol 8:1135.
559 57. Dodsworth JA, Blainey PC, Murugapiran SK, Swingley WD, Ross CA, Tringe SG, Chain
560 PSG, Scholz MB, Lo C-C, Raymond J, Quake SR, Hedlund BP. 2013. Single-cell and
561 metagenomic analyses indicate a fermentative and saccharolytic lifestyle for members of the

562 OP9 lineage. Nat Commun 4:1854.

563 58. Nobu MK, Dodsworth JA, Murugapiran SK, Rinke C, Gies EA, Webster G, Schwientek P,
564 Kille P, Parkes RJ, Sass H, Jørgensen BB, Weightman AJ, Liu W-T, Hallam SJ, Tsiamis G,
565 Woyke T, Hedlund BP. 2016. Phylogeny and physiology of candidate phylum "Atribacteria"
566 (OP9/JS1) inferred from cultivation-independent genomics. ISME J 10:273–8

567

Table 1. Location and description of sampling sites. Temperature and pH were measured in situ *with a hand-held probe.*

Site	Location	Coordinates	Description	pH	T (°C)
AEX-A	Skógakíll	66°10'2.250 N 16°33'59.687 W	Gas seepage sediment	6,4	35,2
AEX-B	Skógakíll	66°10'8.014 N 16°33'56.422 W	Gas seepage water	6,4	53,3
AEX-C	Skógakíll	66°10'12.029 N 16°33'56.998 W	Mud-mire	ND	30,4
AEX-D	Skógakíll	66°10'9.554 N 16°33'57.793 W	Sand-mud	6,4	19,3
SX-A	Skógalón	66°09.222 N 016°37.089 W	Lagoon sediment	8,5	12,1
SX-B	Skógalón	66°09.244 N 016°37.240 W	Puddle water	8,5	13,4

Table 2. Major physicochemical characteristics[1] of water from the two study sites.

	AEX	SX	
pH at 21°C	7.57 ± 0.31	8.64 ± 0.73	(p = 0.19)
Conductivity at 25°C (μScm^{-1})	8945 ± 728	773 ± 392	(p = 0.005)
DIC (as ppm CO_2)	44.8 ± 31.0	94.5 ± 43.1	(p = 0.32)
SiO_2 (ppm)	147.5 ± 2.1	0.35 ± 0.07	(p = 0.0001)
Na (ppm)	1900 ± 56.6	107.4 ± 57.5	(p = 0.001)
K (ppm)	104.9 ± 18.6	4.01 ± 1.96	(p = 0.02)
Mg (ppm)	24.0 ± 15.9	17.8 ± 10.5	(p = 0.69)
Ca (ppm)	311.5 ± 111.0	17.1 ± 9.0	(p = 0.06)
F (ppm)	0.45 ± 0.13	0.21 ± 0.01	(p = 0.11)
Cl (ppm)	3355 ± 276	169.4 ± 105.5	(p = 0.004)
Br (ppm)	12.2 ± 0.8	0.34 ± 0.31	(p = 0.002)
SO_4 (ppm)	215 ± 76.4	5.13 ± 0.60	(p = 0.06)

[1]Dissolved sulphide was determined on-site by titration with mercuric acetate using dithizone as indicator (Arnórsson et al., 2006). Dissolved inorganic carbon was determined by alkalinity titration and back-titration (Arnórsson et al., 2006). Silica was analysed by colorimetric determination of a silica-molybdate complex at 410 nm. Total dissolved solids were determined by gravimetry. Anions were determined by suppressed ion chromatography. Major metals were analysed by atomic absorption spectrometry.

Table 3. Headspace gas analysis[1] on sediment samples from seepage pockmarks at the two study sites.

	AEX	SX
N_2 [%total]	39.2 (±31.5)	81.2 (±2.62)
O_2 + Ar [%total]	8.46 (±8.53)	14.10 (±5.66)
ppm THCG	5.09×10^{5} ($\pm3.88\times10^{5}$)	0.389×10^{5} ($\pm0.296\times10^{5}$)
CO_2 [%THCG]	99.9 (±0.23)	93.2 (±1.77)
Methane (CH_4) [%THCG]	46.1×10^{-3} ($\pm48.3\times10^{-3}$)	6.78 (±1.66)
Ethane (C_2H_6) [%THCG]	2.60×10^{-3} ($\pm4.50\times10^{-3}$)	0 (±0)
Propane (C_3H_8) [%THCG]	1.03×10^{-3} ($\pm1.79\times10^{-3}$)	0 (±0)
iso-Pentane (i-C_5H_{12}) [%THCG]	18.7×10^{-3} ($\pm32.3\times10^{-3}$)	8.00×10^{-3} ($\pm11.3\times10^{-3}$)
Pentane (n-C_5H_{12}) [%THCG]	73.7×10^{-3} ($\pm127\times10^{-3}$)	49.5×10^{-3} ($\pm70.0\times10^{-3}$)
Benzene (C_6H_6) [%THCG]	3.80×10^{-3} ($\pm6.24\times10^{-3}$)	7.15×10^{-3} ($\pm5.45\times10^{-3}$)
Methane $\delta^{13}C$ [‰]	-26.6	-63.2
CO_2 $\delta^{13}C$ [‰]	-3.3	nd

[1]Samples were extracted in dichloromethane/methanol, deasphaltened in pentane, and analysed by gas chromatography.

Table 4.. Number of predicted operational taxanomic units (OTUs) and alpha diversity metrics as calculated at 25,000 sequences from the two study sites.

	Paired seqs	Reads in OTUs	Predict OTUs	Alpha diversity metrics		
				OTUs	Shannon	Chao1
AEX	2.064.234	307.384	14.019	3.461 ± 623	8,3 ± 0,5	3.980 ± 751
SX	2.121.996	287.753	12.767	3.762 ± 333	9,1 ± 0,2	4.203 ± 504

Table 5. Colony-forming units per gram sample after 7 days at 22°C on selective media.

	OX01	**OX01**	**OX03**	**OX03**	**OX06**	**OX06**
	Aerobic	Anaerobic	Aerobic	Anaerobic	Aerobic	Anaerobic
R2A	1.4×105	2.8×104	5.0×105	2.4×105	1.7×107	5.0×106
Naph	2.0×103	<1×103	<1×103	<1×103	2.5×105	1.0×105
Hex	7.5×104	<1×103	2.0×105	<1×103	>2.5×105	2.0×105
2,4-D	nd	nd	<1×103	<1×103	nd	nd
Mn	9.3×104	5.0×103	2.0×105	<1×103	>2.5×105	7.5×104
9K	<1×103	<1×103	<1×103	<1×103	1.0×103	3.0×103
Gui	nd	nd	nd	nd	1.0×106	3.0×106

Table 6. Bacterial isolates and their taxonomic classification by partial 16S rRNA gene sequencing.

Strains	GenBank accession numbers	EzTaxon classification			
		Class	Order	Family	Genus
SX0206, SX1205	MG575948, MG575949	*Actinobacteria*	*Corynebacteriales*	*Nocardiaceae*	*Rhodococcus*
OX0615	MG575950	´´	*Micrococcales*	*Cellulomonadaceae*	*Oerskovia*
OX0315, OX0319	MG575951, MG575952	´´	´´	*Microbacteriaceae*	*Cryobacterium*
OX0117, OX0308, OX0313	MG575953-MG575955	´´	´´	*Micrococcaceae*	*Arthrobacter*
OX0107	MG575956	´´	´´	´´	*Pseudarthrobacter*
OX0614	MG575957	´´	´´	*Sanguibacteraceae*	*Sanguibacter*
OX0316	MG575958	´´	*Streptomycetales*	*Streptomycetaceae*	*Streptomyces*
OX0104, OX0118	MG575959, MG575960	*Cytophagia*	*Cytophagales*	*Cyclobacteriaceae*	*Algoriphagus*
OX0108, OX0126, OX0312	MG575961-MG575963	´´	´´	´´	*Aquiflexum*
OX0623, OX0125, OX0129, OX0311, OX0122, OX0123, OX0314, OX0127	MG575964-MG575971	*Flavobacteriia*	*Flavobacteriales*	*Flavobacteriaceae*	*Flavobacterium*
OX0625	MG575972	*Sphingobacteria*	*Sphingobacteriales*	*Sphingobacteriaceae*	*Pedobacter*
OX1213, OX2513, OX1505, OX2509, OX1011, OX1604, OX1805, OX1004, OX1006, OX1007, OX1210, OX1212, OX2308, OX2309, OX2506	MG575973 - MG575987	*Bacilli*	*Bacillales*	*Bacillaceae*	*Bacillus*
OX0317	MG575988	´´	´´	´´	*Psychrobacillus*
OX2205, OX0307, OX2310, OX0301, OX0302	MG575989 - MG575993	´´	´´	*Paenibacillaceae*	*Paenibacillus*
OX0310	MG575994	´´	´´	*Planococcaceae*	*Jeotgalibacillus*
OX0626	MG575995	´´	´´	*Staphylococcaceae*	*Staphylococcus*
OX1107, OX1109, OX2515, OX2106, OX2313	MG575996-MG576000	´´	*Lactobacillales*	*incertae sedis*	*Exiguobacterium*
OX0102, OX2008, OX0309	MG576001-MG576003	*Alphaproteobacteria*	*Caulobacterales*	*Caulobacteraceae*	*Brevundimonas*
OX0106, OX1214, OX0119, SX1214	MG576004-MG576007	´´	*Rhizobiales*	*Rhizobiaceae*	*Rhizobium*
OX0632	MG576008	´´	*Rhodobacterales*	*Rhodobacteraceae*	*Cereibacter*
OX1314	MG576009	´´	´´	´´	*Paracoccus*

SX0604	MG576010	´´	*Sphingomonadales*	*Erythrobacteraceae*	*Porphyrobacter*
OX0620	MG576011	´´	´´	*Sphingomonadaceae*	*Sphingobium*
OX1313, OX1403, OX1702, OX1216	MG576012-MG576015	*Betaproteobacteria*	*Burkholderiales*	*Burkholderiaceae*	*Paraburkholderia*
OX0105, OX0120, OX0124	MG576016-MG576018	´´	´´	*Comamonadaceae*	*Acidovorax*
OX0630, OX0321	MG576019, MG576020	´´	´´	´´	*Rhodoferax*
OX0130	MG576021	´´	´´	´´	*Variovorax*
OX0611	MG576022	´´	´´	*incertae sedis*	*Paucibacter*
OX0627	MG576023	´´	*Rhodocyclales*	*Rhodocyclaceae*	*Dechloromonas*
OX0617, OX0622, SX0303, OX0110, OX0112, OX0612	MG576024-MG576029	*Gammaproteobacteria*	*Aeromonadales*	*Aeromonadaceae*	*Aeromonas*
OX0619	MG576030	´´	*Alteromonadales*	*Shewanellaceae*	*Shewanella*
OX1909, OX1208	MG576031-MG576032	´´	*Chromatiales*	*Chromatiaceae*	*Rheinheimera*
OX1012	MG576033	´´	*Enterobacteriales*	*Enterobacteriaceae*	*Escherichia*
OX0103, OX0101	MG576034-MG576035	´´	´´	´´	*Rahnella*
OX0604, OX0606, OX0607	MG576036-MG576038	´´	´´	´´	*Shigella*
OX0601, OX0621	MG576039-MG576040	´´	*Pseudomonadales*	*Moraxellaceae*	*Acinetobacter*
OX1807, OX1808, OX0306, OX0322, OX1110, OX0613, SX0305, SX0307, SX1216, SX0304, OX0631, SX1213, OX0304	MG576041-MG576053	´´	´´	*Pseudomonadaceae*	*Pseudomonas*

Table 7. Fractional abundance of Chloroflexi *classes and orders in the seepage pockmarks microbiomes as determined with amplicon sequencing.*

Class	AEX[1]	SX[1]	Order	AEX[2]	SX[2]
Anaerolineae	**0.42**	**0.63**			
			Anaerolineales	0.31	0.22
			'envOPS12'	**0.21**	**0.43**
			'GCA004'	0.09	0.13
			'SHA-20'	**0.20**	**0.04**
			Others	0.19	0.19
Dehalococcoidia	**0.53**	**0.27**			
			Dehalococcoidales	0.18	0.48
			'GIF9'	0.76	0.32
			'FS117-23B-02'	**0.02**	**0.06**
			Others	0.04	0.14
'Ellin6529'	0.03	0.06			
'S085'	0.02	0.02			
Others	0.00	0.01			

[1]Fraction of *Chloroflexi* paired-end sequences (total of 86,729 paired-end reads). Figures in **bold** indicate a significant difference between the AEX and SX microbiota by a two-tailed two-sample Student's *t*-test ($p<0.05$).

[2]Fraction of class-level paired-end sequences (total of 44,384 paired-end *Anaerolineae* reads and 36,549 paired-end *Dehalococcoidia* reads). Figures in **bold** indicate a significant difference between the AEX and SX microbiota by a two-tailed two-sample Student's *t*-test ($p<0.05$).

Table 8. Fractional abundance of Proteobacteria *classes and orders in the seepage pockmarks microbiomes as determined with amplicon sequencing.*

Class	AEX[1]	SX[1]	Order	AEX[2]	SX[2]
Delta-proteobacteria	**0.43**	**0.23**			
			Syntrophobacterales	**0.27**	**0.55**
			Desulfobacterales	**0.26**	**0.07**
			Myxococcales	0.07	0.08
			Desulfarculales	0.06	0.06
			Desulfuromonadales	**0.06**	**0.04**
			'BCP076'	0.14	0.06
			Others	0.15	0.12
Alpha-proteobacteria	**0.48**	**0.63**			
			Rhizobiales	0.88	0.92
			Rhodobacterales	0.06	0.02
			Others	0.06	0.05
Gamma-proteobacteria	**0.11**	**0.06**			
Beta-proteobacteria	0.06	0.07			
Others	0.02	0.01			

[1]Fraction of *Proteobacteria* paired-end sequences (total of 152,153 paired-end reads). Figures in **bold** indicate a significant difference between the AEX and SX microbiota by a two-tailed two-sample Student's *t*-test ($p<0.05$).

[2]Fraction of class-level paired-end sequences (total of 83,764 paired-end *Deltaproteobacteria* reads and 43,823 paired-end *Alphaproteobacteria* reads). Figures in **bold** indicate a significant difference between the AEX and SX microbiota by a two-tailed two-sample Student's *t*-test ($p<0.05$).

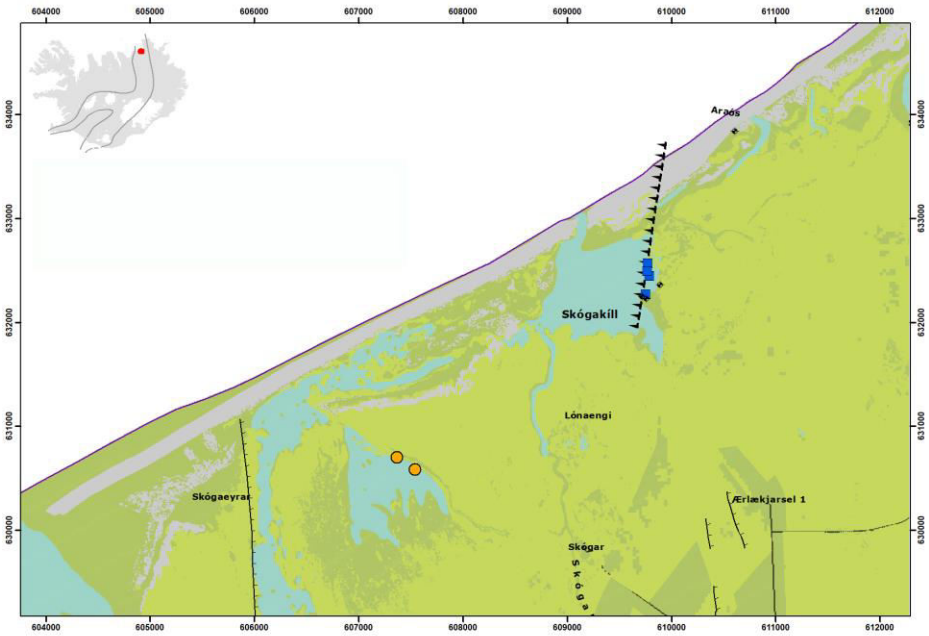

Fig. 1. A map of the study area showing the AEX sampling sites (blue squares) and the SX sites (orange circles). Black diamonds indicate geothermal boreholes. Faults are inferred from the works of Sæmundsson et al. (31) and Ólafsson et al. (18). The insert shows the location of the study area in Iceland and the volcanic rift zone, bounded by the solid lines.

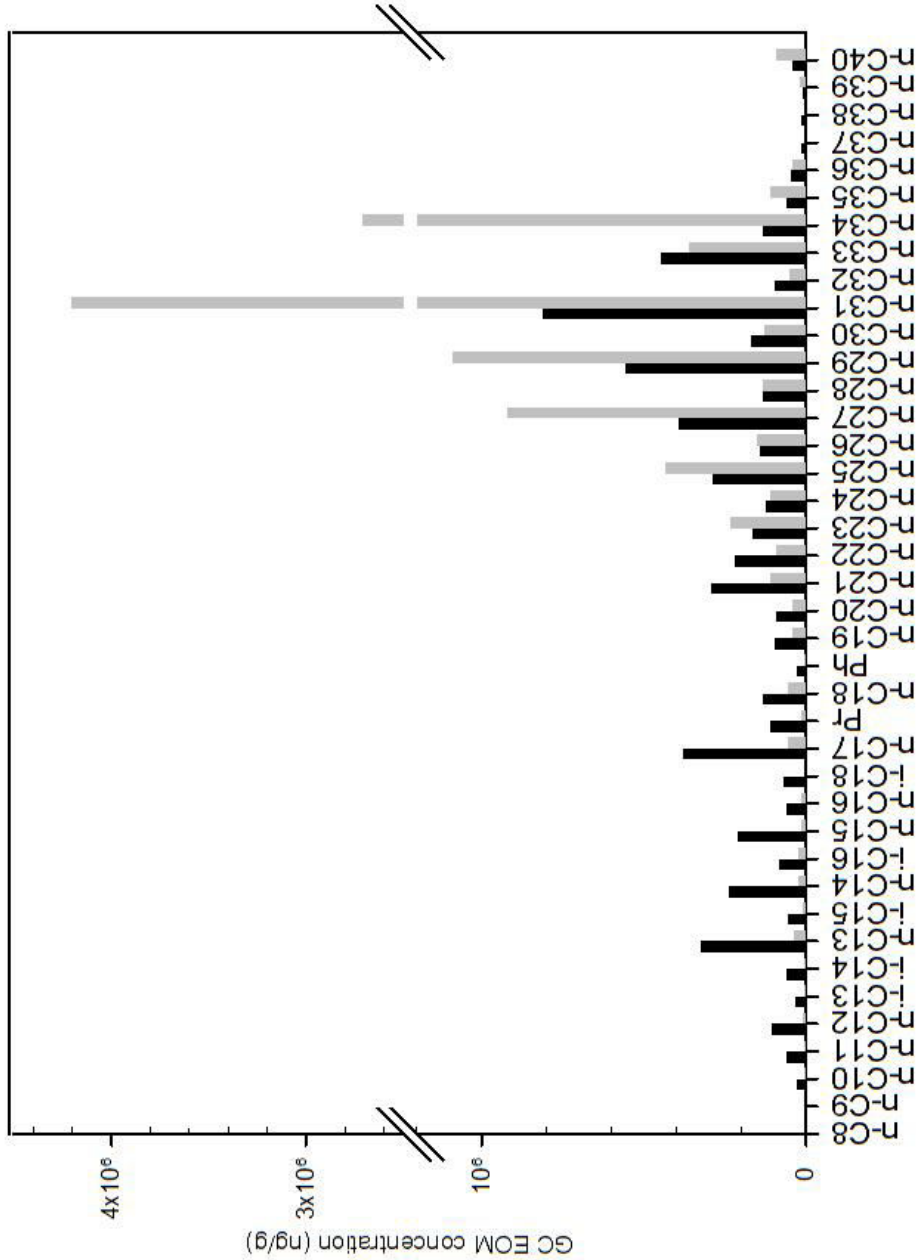

Fig. 2.. Hydrocarbon content in the natural gas seepage pockmarks. Extractable organic matter (EOM) concentration as determined by gas chromatography is compared between the AEX (dark columns) and SX (light columns) study sites. Error bars are omitted for clarity.

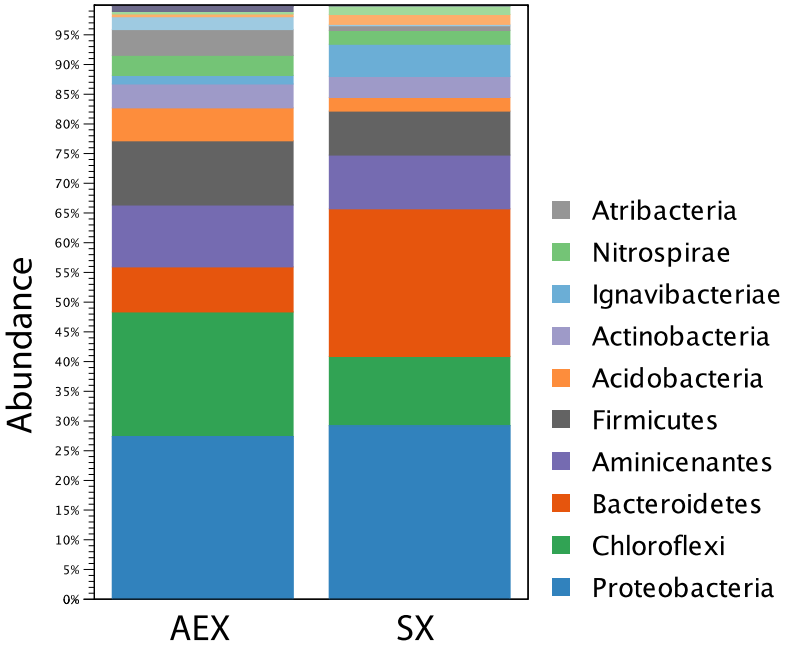

Fig. 3. Bacterial community structure in natural gas seepage pockmarks at Skógakíll (AEX) and Skógalón (SX) sites, presented as the relative abundance of bacterial phyla from amplicon sequencing of V3-V4 in 16S rDNA. Operational taxanomic units (OTUs) with relative abundance lower than 0.1 were omitted.

Table S1. Description of strains, cultured and isolated on differential and selective media, and conserved in 30% glycerol at -70 °C.

Strain no.	Media	T (°C)	Description	Strain no.	Media	T (°C)	Description
OX0101	Naph	22	White	**OX0306**	2,4-D	22	Tan
OX0102	Naph	22	White	**OX0307**	2,4-D	22	Greyish white
OX0103	Naph	22	White	**OX0308**	2,4-D	22	White
OX0104	HEX	22	Pink	**OX0309**	2,4-D	22	White
OX0105	HEX	22	Clear-white	**OX0310**	HEX	22	Tan
OX0106	HEX	22	Yellow, shiny	**OX0311**	HEX	22	Pink
OX0107	HEX	22	White	**OX0312**	HEX	22	Pale pink, flat, somewhat swarmy
OX0108	HEX	22	Pink-clear	**OX0313**	HEX	22	Yellow
OX0109	HEX	22	Pink	**OX0314**	HEX	22	White
OX0110	HEX	22	White, small	**OX0315**	HEX	22	Clear-white, swarming
OX0111	HEX	22	Yellow	**OX0316**	Mn	22	White with a grey centre
OX0112	HEX	22	Clear-white, swarming	**OX0317**	Mn	22	Buff
OX0113	HEX	22	White	**OX0318**	Mn	22	Red
OX0116	Mn	22	White with a grey centre	**OX0319**	R2A	22	Bright yellow
OX0117	Mn	22	bright yellow	**OX0320**	R2A	22	White, irregular
OX0118	Mn	22	Pink	**OX0321**	R2A	22	Bright red
OX0119	Mn	22	snowy white	**OX0322**	R2A	22	Light yellowish brown, irregular
OX0120	Mn	22	Clear-yellow "fried egg"	**OX0323**	R2A	22	Very slightly buff
OX0121	Mn	22	Yellow, shiny	**OX0601**	Naph	22	White
OX0122	R2A	22	Bright orange	**OX0602**	Naph	22	Orange
OX0123	R2A	22	Bright orange	**OX0603**	Naph	22	White, flat
OX0127	R2A	22	Dark yellow	**OX0607**	Naph	22	White

Strain no.	Media	T (°C)	Description	Strain no.	Media	T (°C)	Description
OX0128	R2A	22	White w. dark red peak, coherent	**OX0608**	LAS	22	Snowy white
OX0129	R2A	22	Bright yellow	**OX0611**	HEX	22	White, shiny/oily
OX0130	R2A	22	Pale yellow	**OX0612**	HEX	22	White, shiny/oily
OX0620	Gui	22	bright yellow	**OX1215**	Hex	22°C	Orange
OX0621	Gui	22	White, runny consistency	**OX1216**	BS4 (R2A)*	15°C	Transparent-white, transparent edge
OX0622	Gui	22	Buff, lobate margins	**OX17B03**	R2A	22°C	Very transparent
OX0623	Gui	22	bright yellow	**OX17B05**	R2A	22°C	Light-pink
OX0624	Gui	22	Buff	**OX17B06**	R2A	22°C	Transparent
OX0625	R2A	22	Bright red	**OX1804**	R2A	22°C	Red, crawls a lot
OX0626	R2A	22	Pastel yellow	**OX1805**	R2A	22°C	White-transparent, crawls
OX0627	R2A	22	Yellow "fried egg"	**OX1806**	Hex	22°C	White, round
OX0628	R2A	22	White	**OX1807**	Hex	22°C	Light yellow, slimy
OX0629	R2A	22	Clear-white	**OX1808**	Hex	22°C	Pink
OX0630	R2A	22	Reddish brown	**OX1809**	BS4 (R2A)*	15°	White-transparent, transparent edge
OX0631	R2A	22	Bright yellow with a clear, flat halo	**OX1905**	R2A	22°C	Transparent-White, crawls
OX0632	R2A	22	Pink	**OX1906**	R2A	22°C	White, irregular, crawls
OX0633	R2A	22	Red	**OX1907**	R2A	22°C	Yellow, lighter edge, crawls
OX1004	R2A	22°C	Red, irregular	**OX1908**	Hex	22°C	White, small, irregular
OX1005	R2A	22°C	Small light, crawl much	**OX1909**	Hex	22°C	Transparent, slimy
OX1006	R2A	22°C	Yellow, small, very irregular	**OX2005**	R2A	22°C	Very light-yellow, crawls, small
OX1007	R2A	22°C	Drab (yellow-ish even), irregular	**OX2006**	R2A	22°C	Light-drab, small, crawls alot
OX1008	R2A	22°C	Light-orange, crawls	**OX2007**	R2A	22°C	Orange, crawls a lot, lighter edge

Strain no.	Media	T (°C)	Description	Strain no.	Media	T (°C)	Description
OX1011	Hex	15°C	White	**OX2103**	R2A	22°C	Light-transparent
OX1012	BS4 (R2A)*	35°C	White-transparent, small	**OX2104**	R2A	22°C	White-transpaeant, crawls a lot
OX1105	R2A	22°C	Small, transparent, round	**OX2105**	R2A	22°C	Yellow, crawls
OX1106	R2A	22°C	Small, drab (yellow-ish)	**OX2106**	Hex	22°C	Orange, round
OX1107	R2A	22°C	Light-orange, lighter irregular edge	**OX2107**	Hex	22°C	Light-orange, round
OX1211	R2A	22°C	Yellow, very irregular, lighter edge	**OX1502**	R2A	22°C	Drab, regular, thin edge
OX1212	R2A	22°C	White, round	**OX1503**	R2A	22°C	Creamy, irregular edge
OX1213	R2A	22°C	Orange, very irregular, lighter edge	**OX1504**	R2A	22°C	Drab, crawls
OX1214	Hex	22°C	White, small	**OX1505**	Hex	15°C	Very light orange, small
OX1602	R2A	22°C	White-transparent, thin edge	**SX1204**	R2A	22°C	Light-tranparent, transparent edge
OX1603	R2A	22°C	Yellow, regular, stuck to the agar	**SX1205**	R2A	22°C	Light-pink, cramped, crawls a lot
OX1604	Hex	15°C	White, small	**SX1206**	R2A	22°C	Light-pink, small
OX1702	R2A	22°C	Creamy, transparent, irregular edge	**SX1208**	Hex	22°C	Light-transparent
OX2208	R2A	22°C	Light-orange, crawls	**SX1209**	Hex	22°C	Light orange, round
OX2209	Hex	22°C	White, small, crawls	**SX1210**	Hex	22°C	Light-white, small
OX2210	Hex	22°C	White, small	**SX1212**	Hex	22°C	White, round
OX2305	R2A	22°C	Light-transparent, crawls	**SX1213**	Hex	22°C	White, very slimy
OX2307	R2A	22°C	Orange, lighter edge, irregular	**SX1214**	Hex	22°C	White-transparent, small
OX2308	R2A	22°C	Orange, round	**SX1215**	Hex	22°C	Light-drab, round
Strain no.	**Media**	**T (°C)**	**Description**	**Strain no.**	**Media**	**T (°C)**	**Description**

OX2309	R2A	22°C	Red-pink, round, lighter edge	**SX201**	R2A	22°C	White-transparent, crawls a lot
OX2310	R2A	22°C	White w/ zone	**SX202**	R2A	22°C	Light-transparent-yellow, crawls
OX2311	R2A	22°C	Orange, shines, crawls	**SX203**	R2A	22°C	Pink, crawls, slimy
OX2312	R2A	22°C	Light-transparent, crawls	**SX204**	R2A	22°C	Light-pink, big transparent edge
OX2313	Hex	22°C	Orange, slimy, transparent	**SX301**	R2A	22°C	Light-pink, big, slimy
OX2314	BS4 (R2A)*	22°C	White-transparent, transparent edge	**SX504**	R2A	22°C	White, irregular, crawls a lot
OX2404	R2A	22°C	Light-yellow, crawls	**SX601**	R2A	22°C	White, lighter edge, crawls a lot
OX2405	R2A	22°C	Light semi-transparent, crawls	**SX602**	R2A	22°C	White, crawls
OX2406	Hex	22°C	Light-orange, irregular	**SX0505**	Hex	22°C	Pink, round
OX2514	Hex	22°C	Light orange	**SX1201**	R2A	22°C	White, crawls a lot
OX2515	Hex	22°C	Orange	**SX1202**	R2A	22°C	Shiny white, crawls
OX2516	9K (R2A)*	15°	Very light-pink, small, round	**SX0501**	R2A	22°C	Light-pink, lighter edge, slimy
SX0302	R2A	22°C	Light-white, crawls (long branches)	**SX0502**	R2A	22°C	Pink, crawls
SX0303	Hex	22°C	Transparent	**SX0503**	R2A	22°C	Dark-yellow, crawls a lot, very slimy
SX0304	Hex	22°C	White, small , round				

Table S2. Taxanomic assignment of strains identified by 16S rDNA sequencing and their GenBanka ccession numbers.

Strain	EzTaxon assignemnt	Seq. length	GenBank accession number	%ID	Order	Site[1]
Alphaproteobacteria						
OX0102	*Brevundimonas bullata*	636	MG576001	99.8	Caulobacterales	SX
OX0309	*Brevundimonas bullata*	1394	MG576003	99.9	Caulobacterales	SX
OX2008	*Brevundimonas halotolerans*	1423	MG576002	98.9	Caulobacterales	AEX
SX0604	*Porphyrobacter colymbi*	349	MG576010	98.6	Sphingomonadales	SX
OX0620	*Sphingobium xenophagum*	1451	MG576011	99.4	Sphingomonadales	SX
OX0106	*Rhizobium selenitireducens*	804	MG576004	99.9	Rhizobiales	SX
OX0119	*Rhizobium selenitireducens*	1131	MG576007	99.9	Rhizobiales	SX
OX1214	*Rhizobium sphaerophysae*	872	MG576006	98.1	Rhizobiales	AEX
SX1214	*Rhizobium selenitireducens*	1447	MG576005	97.3	Rhizobiales	SX
OX1314	*Paracoccus homiensis*	721	MG576009	98.1	Rhodobacterales	AEX
OX0632	*Cereibacter changlensis*	1396	MG576008	99.9	Rhodobacterales	SX
Betaproteobacteria						
OX0105	*Acidovorax radicis*	744	MG576016	98.8	Burkholderiales	SX
OX0120	*Acidovorax radicis*	1472	MG576017	99.7	Burkholderiales	SX
OX0124	*Acidovorax radicis*	1380	MG576018	99.5	Burkholderiales	SX
OX0611	*Paucibacter toxinivorans*	1441	MG576022	97.9	Burkholderiales	SX
OX1216	*Paraburkholderia fungorum*	1404	MG576015	99.9	Burkholderiales	AEX
OX1313	*Paraburkholderia fungorum*	1489	MG576012	99.9	Burkholderiales	AEX
OX1403	*Paraburkholderia fungorum*	1492	MG576013	100	Burkholderiales	AEX
OX1702	*Paraburkholderia fungorum*	959	MG576014	100	Burkholderiales	AEX
OX0630	*Rhodoferax fermentans*	1360	MG576019	98.5	Burkholderiales	AEX
OX0321	*Rhodoferax saidenbachensis*	1440	MG576020	99.3	Burkholderiales	AEX
OX0130	*Variovorax*	1465	MG576021	99.4	Burkholderiales	AEX

	ginsengisoli					
OX0627	*Dechloromonas hortensis*	1501	MG576023	98.8	Rhodocyclales	SX
Gammaproteobacteria						
OX0110	*Aeromonas popoffii*	1122	MG576027	99.8	Aeromonadales	SX
OX0112	*Aeromonas popoffii*	1506	MG576028	99.7	Aeromonadales	SX
OX0612	*Aeromonas popoffii*	1451	MG576029	99.7	Aeromonadales	SX
OX0622	*Aeromonas hydrophila*	960	MG576025	100	Aeromonadales	SX
SX0303	*Aeromonas piscicola*	876	MG576026	100	Aeromonadales	SX
OX0617	*Aeromonas cavernicola*	721	MG576024	100	Aeromonadales	SX
OX0631	*Pseudomonas pictorum*	1517	MG576051	99.2	Pseudomonadales	SX
OX1807	*Pseudomonas aestusnigri*	671	MG576041	99.4	Pseudomonadales	AEX
OX1808	*Pseudomonas anguillisepticum*	1536	MG576042	97.9	Pseudomonadales	AEX
OX0306	*Pseudomonas extremaustralis*	1429	MG576043	99.7	Pseudomonadales	AEX
OX0322	*Pseudomonas extremaustralis*	1342	MG576044	99.7	Pseudomonadales	AEX
OX1110	*Pseudomonas guineae*	1502	MG576045	99.8	Pseudomonadales	AEX
OX0613	*Pseudomonas linyingensis*	1450	MG576046	99.9	Pseudomonadales	AEX
SX0305	*Pseudomonas mandelii*	1416	MG576047	99.9	Pseudomonadales	SX
SX0307	*Pseudomonas mandelii*	1503	MG576048	99.9	Pseudomonadales	SX
SX1216	*Pseudomonas mandelii*	1503	MG576049	99.9	Pseudomonadales	SX
SX0304	*Pseudomonas peli*	702	MG576050	99.5	Pseudomonadales	SX
SX1213	*Pseudomonas vancouverensis*	1500	MG576052	99.7	Pseudomonadales	SX
OX0304	*Pseudomonas veronii*	702	MG576053	99.6	Pseudomonadales	SX
OX0601	*Acinetobacter pakistanensis*	1501	MG576039	100	Pseudomonadales	SX
OX0621	*Acinetobacter pakistanensis*	839	MG576040	100	Pseudomonadales	SX
OX0619	*Shewanella putrefaciens*	1511	MG576030	99.5	Alteromonadales	SX
OX0103	*Rahnella aquatilis*	576	MG576034	**94.4**	Enterobacteriales	SX
OX0101	*Rahnella inusitata*	1507	MG576035	99.7	Enterobacteriales	SX
OX0604	*Shigella flexneri*	1505	MG576036	99.7	Enterobacteriales	SX

OX0606	*Shigella flexneri*	1510	MG576037	99.7	Enterobacteriales	SX
OX0607	*Escherichia coli*	858	MG576038	99.5	Enterobacteriales	SX
OX1012	*Escerichia fergusonii*	1504	MG576033	99.7	Enterobacteriales	AEX
OX1208	*Rheinheimera soli*	1515	MG576032	99.0	Chromatiales	AEX
OX1909	*Rheinheimera aestuari*	977	MG576031	99.1	Chromatiales	AEX
Bacilli						
OX0301	*Paenibacillus xylanexedens*	1214	MG575992	98.8	Bacillales	SX
OX0302	*Paenibacillus xylanexedens*	1510	MG575993	99.7	Bacillales	SX
OX2310	*Paenibacillus tundrae*	1497	MG575991	99.3	Bacillales	AEX
OX0307	*Paenibacillus terrae*	1502	MG575990	98.9	Bacillales	SX
OX2205	*Paenibacillus alba*	961	MG575989	99.7	Bacillales	AEX
OX0310	*Jeotgalibacillus campisalis*	1484	MG575994	99.4	Bacillales	SX
OX0626	*Staphylococcus argentus*	1409	MG575995	99.9	Bacillales	SX
OX0317	*Psychrobacillus psychrodurans*	1496	MG575988	99.5	Bacillales	SX
OX1213	*Bacillus aquimaris*	1507	MG575973	99.5	Bacillales	AEX
OX2513	*Bacillus halmapalus*	872	MG575974	98.8	Bacillales	AEX
OX1505	*Bacillus hwajinpoensis*	1262	MG575975	99.0	Bacillales	AEX
OX2509	*Bacillus hwajinpoensis*	1282	MG575976	99.4	Bacillales	AEX
OX1011	*Bacillus oceanisediminis*	937	MG575977	100	Bacillales	AEX
OX1604	*Bacillus oceanisediminis*	363	MG575978	99.2	Bacillales	AEX
OX1805	*Bacillus safensis*	885	MG575979	99.6	Bacillales	AEX
OX1004	*Bacillus vietnamensis*	1434	MG575980	99.9	Bacillales	AEX
OX1006	*Bacillus vietnamensis*	1351	MG575981	99.9	Bacillales	AEX
OX1007	*Bacillus vietnamensis*	1508	MG575982	99.9	Bacillales	AEX
OX1210	*Bacillus vietnamensis*	1394	MG575983	99.8	Bacillales	AEX
OX1212	*Bacillus vietnamensis*	1509	MG575984	99.9	Bacillales	AEX
OX2308	*Bacillus vietnamensis*	1205	MG575985	99.8	Bacillales	AEX

OX2309	*Bacillus vietnamensis*	1059	MG575986	99.7	Bacillales	AEX
OX2506	*Bacillus vietnamensis*	1374	MG575987	99.9	Bacillales	AEX
OX2515	*Exiguobacterium oxidotolerans*	861	MG575998	99.8	Lactobacillales	AEX
OX2106	*Exiguobacterium profundum*	754	MG575999	99.9	Lactobacillales	AEX
OX2313	*Exiguobacterium profundum*	1053	MG576000	99.4	Lactobacillales	AEX
OX1107	*Exiguobacterium profundum*	809	MG575996	99.5	Lactobacillales	AEX
OX1109	*Exiguobacterium profundum*	1463	MG575997	98.2	Lactobacillales	AEX
Flavobacteria						
OX0623	*Flavobacterium glaciei*	992	MG575964	99.0	Flavobacteriales	SX
OX0125	*Flavobacterium granuli*	1446	MG575965	97.8	Flavobacteriales	SX
OX0129	*Flavobacterium granuli*	1449	MG575966	97.8	Flavobacteriales	SX
OX0311	*Flavobacterium hydatis*	1506	MG575967	97.6	Flavobacteriales	SX
OX0314	*Flavobacterium succinians*	1496	MG575970	98.4	Flavobacteriales	SX
OX0122	*Flavobacterium succinians*	1451	MG575968	98.5	Flavobacteriales	SX
OX0123	*Flavobacterium succinians*	1402	MG575969	98.4	Flavobacteriales	SX
OX0127	*Flavobacterium terrigena*	1447	MG575971	98.6	Flavobacteriales	SX
Cytophagia						
OX0104	*Algoriphagus alkaliphilus*	1481	MG575959	97.9	Cytophagales	SX
OX0118	*Algoriphagus alkaliphilus*	1471	MG575960	97.5	Cytophagales	SX
OX0108	*Aquiflexum balticum*	1060	MG575961	**94.7**	Cytophagales	SX
OX0126	*Aquiflexum balticum*	1459	MG575962	**95.5**	Cytophagales	SX
OX0312	*Aquiflexum balticum*	1459	MG575963	**95.5**	Cytophagales	SX
Sphingobacteria						
OX0625	*Pedobacter ruber*	1452	MG575972	98.5	Sphingobacteriales	SX
Actinobacteria						
OX0615	*Oerskovia*	1353	MG575950	98.4	Micrococcales	SX

	paurometabola					
OX0315	*Cryobacterium arcticum*	1463	MG575951	99.3	Micrococcales	SX
OX0319	*Cryobacterium arcticum*	932	MG575952	100	Micrococcales	SX
OX0117	*Arthrobacter alpinus*	1471	MG575953	99.0	Micrococcales	SX
OX0308	*Arthrobacter humicola*	1460	MG575954	99.9	Micrococcales	SX
OX0313	*Arthrobacter oryzae*	1494	MG575955	99.3	Micrococcales	SX
OX0107	*Pseudarthrobacter siccitolerans*	1487	MG575956	99.0	Micrococcales	SX
OX0614	*Sanguibacter suarezii*	1243	MG575957	99.1	Micrococcales	SX
OX0316	*Streptomyces clavifer*	1156	MG575958	99.6	Streptomycetales	SX
SX1205	*Rhodococcus globerulus*	1294	MG575949	99.7	Corynebacteriales	SX
SX0206	*Rhodococcus globerulus*	1482	MG575948	99.7	Corynebacteriales	SX

[1] *Site SX is at Skógaeyralón (66.15°N, 16.62°W). Vegetated, wetland area. Some suspected gas seepage, but little or no evidence of geothermal influence. Site AER is at Skógakíll near Ærlækjarsel (66.17°N, 16.57°W). Mostly barren, sandy, estuarine area characterized by geothermal activity.*